ELSEVIER

Deep-Sea Research II 50 (2003) 3017–3039

DEEP-SEA RESEARCH
PART II

www.elsevier.com/locate/dsr2

Biogeochemical impacts due to mesoscale eddy activity in the Sargasso Sea as measured at the Bermuda Atlantic Time-series Study (BATS)

Erin N. Sweeney[a,b], Dennis J. McGillicuddy Jr.[c,*], Ken O. Buesseler[d]

[a] *MIT/WHOI Joint Program, Massachusetts Institute of Technology, Cambridge, MA 02139, USA*
[b] *Woods Hole Oceanographic Institution, Woods Hole, MA 02543, USA*
[c] *Department of Applied Ocean Physics and Engineering, Woods Hole Oceanographic Institution, Woods Hole, MA 02543, USA*
[d] *Department of Marine Chemistry and Geochemistry, Woods Hole Oceanographic Institution, Woods Hole, MA 02543, USA*

Received 30 July 2002; received in revised form 17 April 2003; accepted 15 July 2003

Abstract

A comparison of monthly biogeochemical measurements made from 1993 to 1995, combined with hydrography and satellite altimetry, was used to assess the impacts of nine eddy events on primary productivity and particle flux in the Sargasso Sea. Measurements of primary production, thorium-234 flux, nitrate + nitrite, and photosynthetic pigments made at the US JGOFS Bermuda Atlantic Time-series Study (BATS) site were used. During the 3 years of this study, four out of six high thorium-234 flux events occurred during the passage of an eddy. Primary production nearly as high as the spring bloom maximum was observed in two mode-water eddies (May 1993 and July 1995). The 1994 spring bloom at BATS was suppressed by the passage of an anticyclone. Distinct phytoplankton community shifts were observed in mode-water eddies, which had an increased percentage of diatoms and dinoflagellates, and in cyclones, which had an increased percentage of *Synechococcus*. These variations in species composition within mode-water eddies and cyclones may be associated with the ages of the sampled eddies, and/or differences in physical, chemical, and biological factors in these two distinct eddy types. In general, eddies that were 1–2 months old elicited a large biological response; eddies that were 3 months old may show a biological response and were accompanied by high thorium flux; eddies that were 4 months old or older did not show a biological response or high thorium flux. A conceptual model depicting temporal changes during eddy upwelling, maturation, and decay can explain the observations in all seven upwelling eddies present in the time-series investigated herein.

1. Introduction

Mesoscale eddies are ubiquitous in the ocean and introduce spatial heterogeneity and temporal variability into a study region. Eddy-driven processes have been implicated in the export of organic material in several regions (e.g. Newton et al., 1994; Honjo et al., 1999; also see the review by Beaulieu, 2002). With the objective of understanding their impact on biogeochemical cycling, we selected already available Eulerian measurements taken at the Bermuda Atlantic Time-series Study (BATS) site located in the Sargasso Sea. The

*Corresponding author. Tel.: +1-508-289-2683; fax: +1-508-457-2194.
E-mail address: dmcgillicuddy@whoi.edu (D.J. McGillicuddy Jr.).

0967-0645/$ - see front matter © 2003 Elsevier Ltd. All rights reserved.
doi:10.1016/j.dsr2.2003.07.008

BATS program was designed to measure seasonal and interannual variability in biogeochemical parameters, and measurements have been taken there since 1988 (Michaels et al., 1994a; Michaels and Knap, 1996; Steinberg et al., 2001). To assess the impact of eddies on these data, we combined the BATS observations with satellite data and a model of eddy activity. Measurements of export flux (using the ^{234}Th technique), nitrate + nitrite concentration, primary productivity, and photosynthetic pigments taken at the BATS site between January 1993 and December 1995 were compared to eddy activity as predicted from dynamic height, potential density, and satellite altimetry data. Eddies have been demonstrated to be important features in the Sargasso Sea (Doney, 1996; McNeil et al., 1999; McGillicuddy et al., 1999). Some studies indicate that eddies contribute significantly to regional biogeochemical budgets (e.g. McGillicuddy et al., 1998, 2003; Siegel et al., 1999), whereas others suggest that eddies play a more minor role (e.g. Oschlies and Garcon, 1998; Oschlies, 2002). Therefore it is essential to understand the impact of these eddies in order to parameterize them in general circulation models and to predict their effects on the calculation of chemical budgets and on the biological activity. This paper investigates the linkage between mesoscale physical disturbances and export.

2. Background

2.1. The BATS station and its seasonal cycle

The BATS station is located near Bermuda in the North Atlantic subtropical gyre at 31°50′N, 64°10′W. The monthly to semimonthly sampling program commenced in October 1988, and consists of both "core" and "bloom" cruises. The period from 1993 to 1995 included 36 "core" cruises and 13 "bloom" cruises. A series of 30 measurements (see Michaels and Knap, 1996, Table 3) were made on the core cruises. Bloom cruises differed in that they did not include sediment trap fluxes and in situ measurements were made only from the surface to 250 m. Bloom cruises also took place two weeks after BATS core cruises in January, February, March and April. BATS measurements of dissolved nitrate + nitrite, primary productivity, photosynthetic pigments, and hydrography are utilized herein. The ^{234}Th fluxes are ancillary to the BATS program and were made only on BATS cruises between 1993 and 1995. The time period of January 1993 to December 1995 is selected for our study to correspond to the ^{234}Th data set because an important emphasis of this work is on the impact of mesoscale eddies on particle flux.

The BATS site is in an area of strong meridional gradients in which seasonal effects have a significant influence on biogeochemistry. This seasonal cycle is described in Michaels et al. (1994a). Typically, the formation of a deep mixed layer of ~150–250 m occurs in February or March of each year (Michaels et al., 1994a; Michaels and Knap, 1996). The entrainment of the deeper nutrient rich waters stimulates a phytoplankton bloom that typically occurs in March and is characterized by increased pigments, biomass, primary production, and particulate organic matter. A shallow, well-stratified mixed layer is present in the summer and fall, until cooling reinitiates the process of deep mixing. Significant variability occurs in the depth of winter mixing and this impacts the strength of the spring bloom in terms of pigment concentration, particulate carbon, nutrient concentrations, and primary production (Lohrenz et al., 1992; Michaels and Knap, 1996; Steinberg et al., 2001).

2.2. Three types of mesoscale eddies

There are at least three types of mesoscale eddies common in the Sargasso Sea (McGillicuddy et al., 1999): cyclones, anticyclones, and mode-water eddies (Fig. 1). Cyclones are marked by cold-water anomalies; they elevate isopycnal surfaces but depress the sea surface due to the higher density of the water circulating within the eddy. Anticyclones have the opposite effect; they are marked by warm-water anomalies, depress the isopycnal surfaces, and elevate the sea surface due to the lower density of the water circulating within this eddy type. Mode-water eddies appear as elevations of the sea surface but have lens-shaped isopycnals, by virtue of upward displacement of

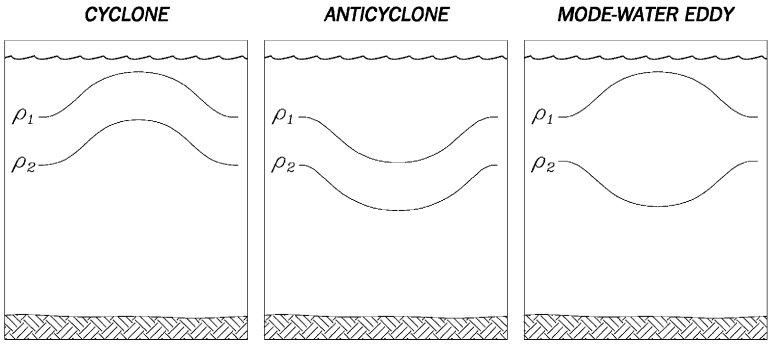

	Cyclone	Anticyclone	Mode-water Eddy
T_{surf}	Decreased	Increased	Decreased
SLA	Depressed	Elevated	Elevated
Rotation	CCW	CW	CW
Isopycnal displacements	Upwelling	Downwelling	Upwelling

Fig. 1. Schematic depiction of the isopycnal displacements of three eddy types in the Sargasso Sea. ρ_1 and ρ_2 correspond to the seasonal thermocline and the main thermocline, respectively. The sense of rotation (CW = clockwise; CCW = counterclockwise) and the impacts of the eddies on upper ocean temperature (T_{surf}), sea level anomaly (SLA), and isopycnal displacements (upwelling vs. downwelling at the base of the euphotic zone) are indicated.

the seasonal thermocline and downward displacement of the main thermocline. Because the main thermocline perturbation dominates the geostrophic flow, these eddies are anticyclonic but, in contrast to other anticyclones, they are associated with a cold-water anomaly near the surface. In the mode-water eddies observed at the BATS site, the direction of the isopycnal displacement in the upper ocean is the same as in a cyclonic eddy. Therefore, the cyclone and mode-water eddies both elevate isopycnals in the upper ocean and cause upwelling into the euphotic zone when they are either forming or intensifying.

2.3. The impact of community structure on particulate export

A biological response is expected to occur as a result of the upwelling of nutrients described above in the presence of a cyclonic or mode-water eddy. This response may include increased productivity and increased particle flux as well as a planktonic community structure shifts (Wiebe and Joyce, 1992; Olaizola et al., 1993; Brzezinski et al., 1998; McNeil et al., 1999; Scharek et al., 1999a, b; Letelier et al., 2000; Seki et al., 2001; Savidge and Williams, 2001). Both productivity and plankton community structure impact biological export of carbon to the deep ocean. Therefore, the factors that control the dynamics of the upper ocean are essential to understanding the efficiency of the biological carbon pump. Sinking particles can be comprised of aggregated small organisms and other detrital material, biomass of larger organisms, and fecal pellets. At BATS, an average of 39% of the carbon flux is comprised of fecal pellets, whereas in the oligotrophic Pacific (Hawaii Ocean Time-series program's Station ALOHA) fecal pellets appear to comprise ~100% of the carbon flux (Roman et al., 2002). By affecting the quantity and composition of surface particles, the size distribution and species composition of phytoplankton appears to be of great importance in controlling the carbon export from the surface ocean (Archer, 1995; Michaels and Silver, 1988; Boyd and Newton, 1999).

Carbon export does not appear to be related directly to the rate of primary production. For example, decoupling of primary productivity and export has been observed in the central North Pacific (Karl et al., 1995, 1996), in the Arabian Sea (Buesseler et al., 1998), and at the BATS site

(Michaels and Knap, 1996; Conte et al., 2001). Small phytoplankton taxa (e.g. *Prochlorococcus* and *Synechococcus*), $<5\,\mu m$ in size, are the most abundant primary producers in the open ocean but do not appear to contribute significantly to export (Goldman, 1988, 1993). They may contribute little to export because they are effectively grazed by protozoa within the microbial loop (Glover et al., 1988), they have extremely low sinking rates (Takahashi and Bienfang, 1983), and they are only weakly associated with larger sinking detrital particles (Silver et al., 1986).

Larger phytoplankton (such as diatoms) are believed to be very important to the rate of carbon export (Goldman, 1988, 1993). Boyd and Newton (1995) attributed marked interannual variability in the POC flux associated with 1989 and 1990 spring blooms in the northeast Atlantic to the absence of large diatoms in 1990. Also, in a study of biogenic silica production in the upper water-column at BATS, export of diatoms was estimated to account for 30% of the organic carbon export (Brzezinski and Nelson, 1995) even though they are only estimated to contribute 8% of the primary production (Boyd and Newton, 1999). Table 1 shows common phytoplankton groups and their size classes. In general, diatoms and dinoflagellates are considered the major contributors to the large size fraction at the BATS site (Andersen et al., 1996).

The importance of diatoms and other large phytoplankton to flux is due to many factors. First, larger organisms have higher sinking rates. In addition to their larger size, diatoms produce a silica frustule, which gives them a higher density than other phytoplankton and can cause them to sink more rapidly out of the upper ocean. The enhanced ballasting effects of $CaCO_3$ have likewise been proposed to promote sinking fluxes to the deep ocean interior (Armstrong et al., 2002; Francois et al., 2002). Also, fast-growing diatoms isolated from the Sargasso Sea were observed to produce giant flocculent masses that would be expected to further increase the size and thus the sinking rate (Goldman, 1993). Second, larger phytoplankton promote short food webs that lead to larger grazers and thus larger sinking particles (Michaels and Silver, 1988). Also, large phytoplankton cells contain many times the carbon content of small cells; for example, $\sim 5 \times 10^4$ cyanobacteria equal the carbon content of one 100 μm round (equivalent spherical diameter) diatom (Goldman, 1988).

While food web controls on particle export have been identified, quantifying upper-ocean particle fluxes remains a difficult task. This is in part due to the problems associated with direct methods of catching sinking particles in the upper ocean using sediment traps, which may include: hydrodynamic biases; non-passive fluxes associated with "swimmers"; and the resolubilization of particles once collected (see review by Gardner, 2000). An alternative approach is to use the naturally occurring radionuclide thorium-234 as an in situ tracer of the sinking flux of particles in the upper ocean, as reviewed in Buesseler (1998) and presented in detail for this study below. At BATS, a comparison of the 3-year record of particle flux derived from ^{234}Th with the measured sediment trap flux shows that the traps did not record any high ^{234}Th flux events (Buesseler et al., 1994, 2000). Similarly, at the Hawaii Ocean Time-series

Table 1
Phytoplankton groups and associated size classes (Jeffrey et al., 1997; Sieburth and Smetacek, 1978)

Phytoplankton group	Typical size	Size class
Prochlorococcus sp.	0.5 μm	Picoplankton
Synechococcus sp.	1 μm	Picoplankton
Prymnesiophytes (includes coccolithophorids)	5–20 μm; 2 mm filaments	Nanoplankton mesoplankton
Prasinophytes	1–40 μm	Nano-microplankton
Pelagophytes	2–3 μm	Pico-nanoplankton
Dinoflagellates	2–200 μm (some up to 2 mm)	Nano-microplankton (some mesoplankton)
Bacillariophytes (diatoms)	2–200 μm (some up to 2–4 mm)	Nano-microplankton (some mesoplankton)

site, ALOHA, a 1-year record shows two large export events derived from time-series ^{234}Th data that were not measured in standard sediment traps (Benitez-Nelson et al., 2001). Inclusion of these events in the annual ALOHA C budget matches more closely other estimates of annual export production at this site. We therefore feel that the dynamics and magnitude of particle export in the upper ocean can be more reliably predicted from the ^{234}Th data, and we rely on ^{234}Th exclusively as our indicator of enhanced particle flux associated with the passage of eddies at BATS.

3. Methods

3.1. Locating and tracking mesoscale eddies

Satellite altimetry measurements from both TOPEX/Poseidon (T/P) and European Remote Sensing (ERS) platforms were used in this study to detect mesoscale eddies. T/P completes its global coverage once every 10 days with ground tracks approximately 250 km apart at the latitude of Bermuda. ERS-1 and ERS-2 complete their cycle of global coverage every 35 days but provide much closer spacing of approximately 70 km.

Observations of the MODE and POLYMODE programs documented eddy sizes in the Sargasso Sea of 100–150 km with the minimum time period for significant changes in mesoscale flows (synoptic dynamical time scale) of 10 to 15 days (Richman et al., 1977; The MODE Group, 1978; Harrison and Heinmiller, 1983). Thus, the T/P and ERS missions occupy opposite ends of the space/time resolution requirements needed for direct diagnosis of mesoscale processes in this region. The T/P repeat cycle can adequately resolve temporal variations in the eddies near Bermuda, but the ground tracks are far enough apart that an entire eddy can fit in between them. Closer spacing of the ERS tracks insures satisfactory spatial coverage, but the repeat cycle is so long that important temporal dynamics can be missed. Therefore, measurements from both T/P and ERS satellites were interpolated using objective analysis to provide daily eddy fields and to diagnose mesoscale fluctuations in the BATS measurements.

The sea-level anomaly (SLA) data used in this study were provided by Archiving, Validation, and Interpretation of Satellite Data in Oceanography (AVISO, 1997). The data of ERS and T/P was merged by AVISO staff using the global minimization algorithm of LeTraon et al. (1995) and LeTraon and Ogor (1998), which provides compatible error characteristics in the data. An accuracy of $\sim$3–5 cm was achieved (AVISO, 1997).

Spatial maps of SLA were obtained by objective analysis of the SLA data. Objective analysis is a statistical data treatment that provides a local estimate of the mean value of a field variable. The method used to generate these field estimates incorporates a prescribed covariance function, which in this case includes time and position, as well as a phase speed for westward propagation. Each field estimate was formed based on a combination of the current SLA and knowledge of the previous and future SLA data. Details of this method are given in Carter and Robinson (1987) and Siegel et al. (1999). Objectively analyzed fields were made on a $\sim$25 km grid in a domain spanning latitude of 28° to 38°N and longitude of 75° to 45°W.

Eddy field animations were generated from the objective analyses (available on line at http://science.whoi.edu/users/mcgillic/tpd/anim.html). These animations were used to identify eddies passing near the BATS site during the period between 1993 and 1995. Features were selected using these animations based on several criteria. First, coherent features with maximum sea level displacements exceeding 10 cm were selected. The error of the SLA analysis along tracks is $\sim$3–5 cm and greater in the areas where data are interpolated; features with a magnitude below 10 cm were not viewed as significantly different from background levels. SLA was corroborated by dynamic height calculations from BATS hydrography. Additional confirmation of a feature was made by examination of hydrographic profiles from BATS, i.e. a vertical displacement of the isopycnal surfaces indicates the presence of an eddy. During times when satellite coverage was

poor and the error in the SLA generated eddy field is high, potential density and dynamic height are considered better indicators of an eddy's presence. High-resolution time-series records from the Bermuda Testbed Mooring (Dickey et al., 1998) also were used when available.

The altimetric fields also were used to examine the temporal evolution of each eddy feature as it move past the BATS site. Changes in the magnitude of each eddy's SLA extremum provided an indicator as to whether the feature was intensifying or decaying at any particular time. In addition, eddy "age" was estimated by tracking each eddy's local SLA extremum as far backward in time as a coherent manifestation of the eddy was observed. Given the repeat cycles of the T/P and ERS altimeters, we estimate the uncertainty in the eddy age assessment to be 0.5 months.

3.2. Thorium-234 activity and flux calculation

The ^{234}Th activity measurements were made in accordance with Buesseler et al. (1994). The sampling program was designed to compare measured ^{234}Th predicted flux to measured values taken from sediment traps at 150 m. Therefore the samples were "vertically integrated" between the surface and 150 m by collecting water at 12 evenly spaced depths in a clean 2-l polycarbonate bottle and combining these samples immediately into a 25-1 polyethylene collapsible container (cubitainer). The accuracy of this volume measurement was $\pm 0.3\%$. Next, 1 ml of 6 disintegrations per minute (dpm) ^{230}Th ml^{-1} was added as a recovery standard, along with 5 ml of $FeCl_2$ in HCl (50 mg ml^{-1} in $FeCl_2$), and 30 ml concentrated HNO_3. Each sample equilibrated for 24–60 h on the ship and was returned to Bermuda Biological Station for Research (BBSR) within 60 h of collection.

At BBSR each sample was weighed and the pH was adjusted to a value of 8 using concentrated NH_4OH. An Fe precipitate formed and served to scavenge the thorium and other particle reactive substances from solution. This Fe precipitate was collected on a GF/F filter and mailed to Woods Hole Oceanographic Institution (WHOI) for further analysis. The Fe precipitate was next dissolved in concentrated HCl and treated using ion exchange purification procedures to separate thorium from the other beta emitters (Fleer, 1991; Buesseler et al., 1992b). Within 4–17 days of collection, the ^{234}Th was separated from its parent ^{238}U by passing it through an ion exchange column in 8 N HCl (10 ml volume, BioRad AG1 × 8 100–200 mesh resin). A second ion exchange column (5 ml, AG1 × 8 resin 100–200 mesh in 8 N HNO_3 form) was then used to purify the thorium from other beta emitters.

The final purified thorium was electroplated onto a stainless steel planchette for low-level beta counting. Each sample was first alpha counted for 48–96 h for ^{230}Th to determine the overall chemical yield. Subsequently, each planchette was mounted with a 9 mg cm^{-2} foil cover, to reduce any low-energy beta emissions, and then counted with a gas flow proportional counter. The beta detectors used had an average background count rate of 0.4–0.5 counts per minute (cpm) (Noshkin and DeAgazio, 1966). Blanks were run to ensure that there was no thorium-234 beta activity in the yield monitor or reagents. ^{234}Pa, a short-lived daughter product of ^{234}Th, has a much stronger beta signal, and it is the primary beta particle measured to quantify the activity of ^{234}Th in each sample. The method was calibrated by taking advantage of the fact that ^{238}U can be predicted from salinity to an accuracy of $\pm 1\%$ (Chen et al., 1986) and that at greater depths, fluxes of ^{234}Th on particles are so low that ^{234}Th reaches secular equilibrium with ^{238}U activity, i.e. $^{234}\mathrm{Th}/^{238}\mathrm{U} = 1.00$ (Buesseler et al., 1994). For improved precision and accuracy, each sample was counted 5–6 times on the same detector for three 500-min cycles over a period of 50–60 days. A decaying activity curve was then fit to these measurements to determine the ^{234}Th activity at the time of sample collection and the total background activity. Measurements requiring large in-growth corrections ($>10\%$) due to the decay of the ^{238}U parent in the sample between collection and purification in the lab, and/or measurements having poor chemical recovery ($<50\%$) of ^{234}Th were not considered statistically accurate and were not used in this study.

Using the measured ^{234}Th activities, export of ^{234}Th on sinking particles can be determined.

^{234}Th ($t_{1/2} = 24.1$ days) is the daughter of ^{238}U decay. Local loss terms for ^{234}Th include radioactive decay and particle flux, owing to the fact that ^{234}Th is very particle reactive. Therefore, an activity balance can be used to determine its flux:

$$\partial^{234}\mathrm{Th}/\partial t = (^{238}\mathrm{U} - {}^{234}\mathrm{Th})\lambda - P + V, \quad (1)$$

where ^{238}U is the uranium activity in sea water, determined from its conservative relationship with salinity according to Chen et al. (1986), ^{234}Th is the measured activity in the water column, λ is the decay constant for ^{234}Th, P is the net export flux of ^{234}Th on sinking particles, and V is the sum of advective and diffusive ^{234}Th fluxes. In this work we have applied a steady state assumption, which assumes that the particle flux has been constant over several weeks preceding the measurement. Due to radioactive in-growth from ^{238}U decay, the measured ^{234}Th activity would be the same with either a large particle flux event which occurred several weeks earlier, or due to a steady period of low thorium flux on sinking particles. To account for time-varying ^{234}Th activities, a non-steady state model can be applied as in Buesseler et al. (1992a) for the North Atlantic bloom experiment; however, we do not have the necessary time-series data to apply a non-steady state model to each eddy sampled here. We can, however, estimate the error introduced from using a steady state assumption by comparing two subsequent monthly ^{234}Th measurements taken within the center and edge of the same eddy. The activity of ^{234}Th was 2.35 dpm l^{-1} in July 1995 (eddy center) and 2.3 dpm l^{-1} in August 1995 (eddy edge). The collection dates differed by 39 days and thus a $\partial^{234}\mathrm{Th}/\partial t$ of 190 dpm m^{-2} d^{-1} can be applied to Eq. (1), giving an approximate 15% error in the August 1995 flux when this term is ignored. This temporal evolution of ^{234}Th within an eddy can thus impact fluxes, but without time-series data within an evolving eddy, we can only approximate from this analysis that the impact on fluxes calculated here assuming steady state will be less than twice this value, or $<30\%$, in both positive and negative directions.

Neglecting advective and diffusive fluxes in Eq. (1) results in additional uncertainties. However, these are usually small compared to the other terms in the ^{234}Th activity balance (Buesseler, 1998). A more complete discussion of the impact of ignoring horizontal and vertical transports on the ^{234}Th activity balance at BATS can be found in Buesseler et al. (1994). However, this earlier study did not consider the impact of eddies on the local ^{234}Th balance. In the case of upwelling, as with a cyclone or mode-water eddy, the flux calculated from Eq. (1) would be lower than the actual flux, since we have ignored the upwelling of ^{234}Th-rich deep waters in the activity balance. We calculate that this may result in an underestimate in the ^{234}Th flux as high as $\sim 20\%$ based on an upper-limit upwelling rate of 1 m d^{-1} (McGillicuddy and Robinson, 1997) and a deep water ^{234}Th activity in secular equilibrium with ^{238}U. In the case of downwelling, assuming replacement through lateral inputs at the surface, and as long as there is not significant horizontal heterogeneity, the ^{234}Th flux would not be effected. Because these corrections are relatively small and difficult to constrain further, advective and diffusive terms were ignored in these thorium flux calculations.

Overall, there are both model and analytical sources of error in any ^{234}Th flux calculation. Because the particle flux in the Sargasso Sea is generally very low, the net flux value (P), represents a small differences in two large numbers, the ^{234}Th and ^{238}U activities. Therefore, the error in the calculated flux is larger than the individual activity errors due to propagation of errors (Coale and Bruland, 1987). Counting statistics alone result in a propagated flux error of ± 200–300 dpm m^{-2} d^{-1}. In addition, because the samples were taken at BATS and analyzed at WHOI, there were several days before processing and as a consequence the difference between measured ^{234}Th activity and its ^{238}U parent decreases due to natural ingrowth of ^{234}Th after sampling. This ingrowth is accounted for in the data reduction, but higher ingrowth still results in larger uncertainties in the ^{234}Th activity at sampling. In addition, logistical constraints required the combination of the water samples between the surface and 150 m, so the difference between ^{234}Th and ^{238}U was decreased again since ^{234}Th is generally lowest between the surface and 50–100 m. As mentioned above, there are inherent

errors in the steady state approximation and in neglecting advection and diffusion. On some cruises, multiple measurements were taken on a cruise and these values were averaged to determine one flux estimate for each cruise. By considering these different sources of uncertainty, we estimate the total error on the ^{234}Th derived flux values to be approximately $\pm 500\,\mathrm{dpm\,m^{-2}\,d^{-1}}$. Given the average value of $540\,\mathrm{dpm\,m^{-2}\,d^{-1}}$ for the time period between 1993 and 1995, we have deemed flux values of greater than approximately twice this value, or $1000\,\mathrm{dpm\,m^{-2}\,d^{-1}}$, as representing significantly elevated export values that will be considered in our discussion below.

3.3. Bermuda Atlantic Time-series Study (BATS) measurements

Details of the sampling scheme, analytical methods and quality control procedures used for BATS measurements are available in the BATS Methods Manual (Knap et al., 1993) and in the literature (Lohrenz et al., 1992; Michaels et al., 1994a, b; Michaels, 1995). All the measurements are available from the BATS web site at http://www.bbsr.edu/users/ctd/batdatex.html.

3.4. Determining community structure from pigment data

Photosynthetic pigment distributions can be used to infer phytoplankton community composition. Table 2 shows pigments that are useful as taxonomic markers. The pigments we have selected for this study are total chlorophyll *a* (monovinyl plus divinyl), chlorophyll *b*, 19′-butanoyloxyfucoxanthin, fucoxanthin, 19′-hexanoyloxyfucoxanthin, peridinin, prasinoxanthin, and zeaxanthin + lutein (the HPLC method employed is not capable of separating lutein from zeaxanthin). Most phytoplankton groups contain monovinyl chlorophyll *a*, however, *Prochlorococcus* contains divinyl chlorophyll *a*. The presence of both chlorophyll *b* and zeaxanthin indicates the presence of *Prochlorococcus*. Chlorophyll *b* and prasinoxanthin indicates prasinophytes. Zeaxanthin without chlorophyll *b* indicates the presence of cyanobacteria such as *Synechococcus* and *Trichodesmium*; for brevity we refer to this group as *Synechococcus* in the text and figures below. An increase in fucoxanthin with corresponding increases in 19′-hexanoyloxyfucoxanthin and/or 19′-butanoyloxyfucoxanthin indicates prymnesiophytes and/or pelagophytes, respectively. For the pigment data to indicate the presence of diatoms, fucoxanthin must increase without corresponding increases in 19′-hexanoyloxyfucoxanthin and 19′-butanoyloxyfucoxanthin (Michaels et al., 1994a). Finally, peridinin is a biomarker for members of the Dinophyceae (dinoflagellates).

Table 2
Summary of important marine phytoplankton taxa and their diagnostic pigment biomarkers (after Andersen et al., 1996)

Phytoplankton group	Diagnostic pigment(s) present
Prochlorococcus sp.	Divinyl chlorophylls *a* and *b*, zeaxanthin
Cyanobacteria	Zeaxanthin
Bacillariophytes (diatoms)	Fucoxanthin
Prymnesiophytes	19′-hexanoyloxyfucoxanthin, fucoxanthin
Pelagophytes	19′-butanoyloxyfucoxanthin, fucoxanthin
Cryptophytes	Alloxanthin
Dinoflagellates	Peridinin
Prasinophytes	Prasinoxanthin
Chlorophytes	Lutein

Algorithms have been developed based on the ratios of different pigments found in representative phytoplankton cultures, to determine the percent chlorophyll *a* contributed by different algal groups (Letelier et al., 1993; Andersen et al., 1996; Mackey et al., 1996, 1998; Wright et al., 2000). We chose to use the one developed for the oligotrophic Pacific by Letelier et al. (1993), justified on the basis that the HPLC signatures of the various phytoplankton groups are generally similar at HOT and BATS (Andersen et al., 1996). We also note that the Letelier et al. (1993) algorithm has been used previously for the BATS site (Boyd and Newton, 1999). Of course, there are a number of limitations inherent in such algorithms. To begin with, the equations (see Table 1 in Letelier et al., 1993) assume that the ratios of different pigments remain constant within algal groups and in organisms under different growth conditions. Also, the equations are based on shade

adapted cultures (light equivalent to roughly 75 m), and they assume that all organisms in a given group have ratios of pigments similar to those used to develop the equations (for example, it is known that at least one type of diatom uses 19′-butanoyloxyfucoxanthin) (Letelier et al., 1993). Because of these assumptions, we will use these equations to provide only a rough approximation of what the changes in pigment concentrations mean in terms of community structure.

4. Results and discussion

The data recorded at BATS allow us to compare indicators of biological activity and geochemical properties to examine the impacts of mesoscale eddies between 1993 and 1995 on the local biogeochemistry at this fixed site. As each eddy passes the BATS site, its impacts on the monthly to semi-monthly measurements are based on many variables. These include the seasonal cycle at BATS, other mixing events (such as storms), the direction of isopycnal displacement, the life cycle of the eddy, and the path of the eddy's center with respect to the location of BATS. Nine eddy events observed during the time period of the study are discussed below (summarized in Table 3). These nine events were selected because they coincide with BATS sampling (i.e. we omitted eddies that passed the site between BATS sampling periods) and the displacement of the sea surface in the center of the eddy (not necessarily at the BATS site) was greater than 10 cm. First, mode-water eddies are discussed, followed by cyclones, and then anticyclones.

To aid in our discussion and analysis of the observations from each eddy we developed a conceptual model depicting the sequence of events and impacts of eddy upwelling (Fig. 2). We tested this model by comparing it with the observations of each eddy event. The model depicts the sequence of events expected to occur in the upper ocean during the lifetime of a mode-water eddy or

Table 3
Summary of the observations for nine eddy events occurring at BATS between 1993 and 1995

ID#	Eddy Type	Date	Com. shift	Int	Nut	Prod	Pig	Th	Age	Model stage
May93	mw	April 1993	pras + pel + diat	↑	↑	—	↑	N/A	1(5)	3
	mw	May 1993	pras + pel + diat	↑	↑	↑	↑	—	1.5(5)	3
Jul95	mw	July 1995	diat + dino	↑	↑	↑	↑	↑	1.5(8)	4
	mw	Aug 1995	—	↓	—	—	—	↑	3(8)	6
Oct95	mw	Sept 1995	—	↓	↑	—	—	—	3(10)	?
	mw	Oct 1995	—	↑?	—	—	—	—	4(10)	7
Jan93	c	Jan 1993	syn	↑	—	—	—	↑	3 + (9 +)	5 or 6?
	c	Feb 1993	syn	↑	↑	—	—	↓	4 + (9 +)	?
Jul93	c	June 1993	syn	↓	—	—	—	↑↑	3(8)	6
	c	July 1993	syn	↓	—	—	—	—	4(8)	7
Nov93	c	Nov 1993	—	↓	↓	—	—	N/A	10(11)	7
Aug94	c	July 1994	syn	↑	↑	—	—	—	2(5)	3
	c	Aug 1994	syn + dino	↓	—	—	↑	↑	3(5)	5
Mar94	anti	Mar 1994	diat + pras	↓	↑	↓	↓	—	9(12)	N/A
Sept94	anti	Sept 1994	—	↓	—	—	—	N/A	5(8)	N/A
	anti	Oct 1994	—	↓	—	—	—	—	6(8)	N/A

Arrows indicate increasing or decreasing, dashes are no significant change from average value, and N/A is no measurement available. ID# corresponds to the labels on the figures of biogeochemical parameters. Eddy type, mw—mode-water, c—cyclone, anti—anticyclone. Com. shift refers to shifts from the typical phytoplankton community structure at BATS with diat—diatoms, pel—pelagophytes, pras—prasinophytes, dino—dinoflagellates, and syn—*Synechococcus*. Int—intensity of eddy, Prod—productivity, Pig—pigment concentrations, Th—thorium-234 flux, Nut—nitrate + nitrite, Age—age of eddy in months at BATS followed by the total age of the eddy in parenthesis with a + symbol meaning the eddy extended beyond the available data period or region, Model stage-represents the eddy's stage in the conceptual model shown in Fig. 2.

cyclone. When the eddy is first forming, little effect is expected (stage 1). On continued intensification, significant amounts of nutrients are upwelled into the euphotic zone (stage 2). This nutrient injection is likely to be followed by increased primary productivity, pigment concentrations, and/or other possible biological responses (stage 3). After some period of time, the biological response is expected to stimulate increased export (stage 4).

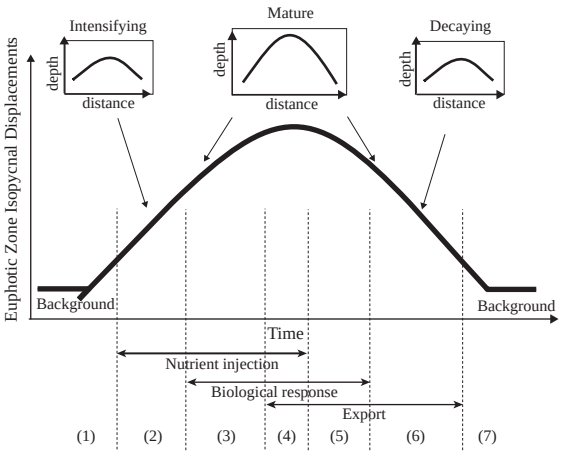

Fig. 2. Conceptual model of the effects of a mode-water eddy or cyclonic eddy on an upper ocean ecosystem. The numbers (1–7) on the bottom of this figure correspond to stages in an eddy's life cycle (see text). The upper panels schematize cross-sections of an eddy, depicting the vertical displacement of an isopycnal as the eddy intensifies, matures, and subsequently decays.

Then, as the eddy begins to decay, the nutrient injection would subside (stage 5). At some time nutrients will be exhausted, productivity decreases, and a high export signal remains due to the longer time scale over which export is averaged by the ^{234}Th tracer (stage 6). Finally, even the thorium signal is expected to disappear as the eddy continues to decay and ^{234}Th returns into equilibrium with its ^{238}U parent (stage 7).

A detailed discussion of the SLA histories of each of the nine eddy events is presented in Sweeney (2001). An example of this work is shown in a group of images depicting the evolution of one of the eddies (Figs. 3 and 4). The eddy is a mode-water eddy and is present at BATS on July 10, 1995 (Fig. 3a) and just west of BATS August 18, 1995 (Fig. 3b). This eddy formed in May 1995, passed over the BATS site in July 1995 (while still intensifying in magnitude) during BATS sampling, and was decaying in strength and west of the site in August (Figs. 3b and 4). Images such as these are available for all nine eddies in Sweeney (2001) and were used to help complete Table 3 of this paper.

To observe the effects of the passage of each eddy, a group of figures depicting physical, chemical, and biological information are presented showing the biogeochemical indicators from January 1993 to December 1995 (Figs. 5–10). These figures are marked with colored bars that correspond to the passage of an eddy; light blue for cyclones, yellow for mode-water eddies, and red

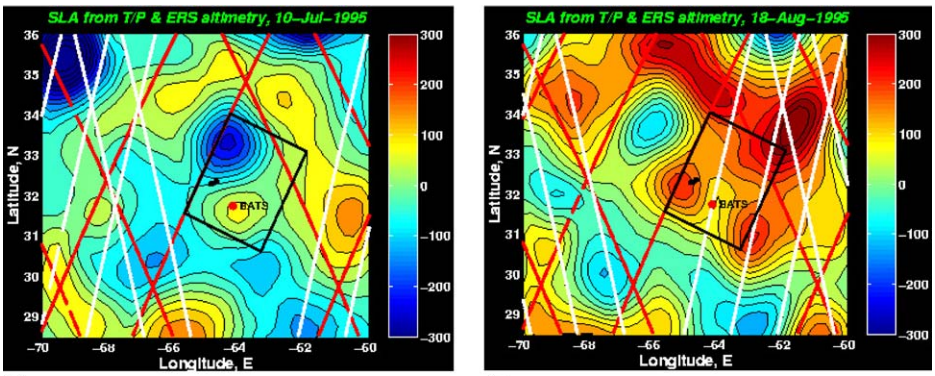

(a) (b)

Fig. 3. Eddy fields for July 10 (a) and August 18 (b) 1995. Image on July 10 shows positive SLA anomaly associated with mode-water centered on BATS and August 18 image shows same eddy intensified west of BATS. Color scales indicate sea level anomaly in millimeters; red and white lines represent satellite passes from Topex/Poseidon and ERS, respectively.

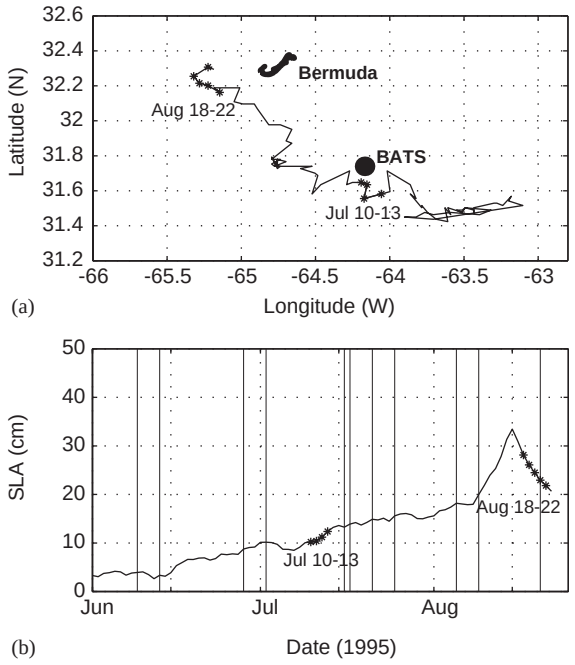

Fig. 4. Map of eddy trajectory (a) and maximum SLA within the eddy feature vs. time (b). Asterisks in panels (a) and (b) indicate the times of sampling at the BATS site, and vertical lines in panel (b) indicate satellite passes through eddy center.

for anticyclones. In addition, green bars indicate peaks in productivity that are not associated with eddies. Of these non eddy-related features, March 1993 and 1995 are spring blooms and May 1995 is due to weather related deep mixing (S. Doney, pers. comm.). To compare the monthly measurements and to help establish typical conditions at BATS during this time period we calculated the average values of all measurements of integrated primary productivity, thorium flux, and phytoplankton community composition; these average values are shown as dashed lines on the relevant figures.

During this 3-year period, prymnesiophytes, pelagophytes, and *Prochlorococcus* most often dominate the phytoplankton community. The variability in the prymnesiophytes contribution to chlorophyll *a* is small; the value remains close to its average throughout the time-series and does not respond to the passage of eddies (Fig. 10). In the case of *Prochlorococcus*, its contribution to total chlorophyll *a* is seasonally dependent, being highest in the fall and lowest during spring blooms. This result agrees with the findings of DuRand et al. (2001) based on flow cytometry, which document a seasonal cycle of *Prochlorococcus* in cell concentration and percent phytoplankton carbon. Chlorophyll *a* contributions from *Synechococcus*, prasinophytes, dinoflagellates, and diatoms are more variable relative to the three other phytoplankton groups described above. It should be noted, however, that the values shown in Fig. 10 are expressed as percent chlorophyll *a*, a parameter that does not necessarily reflect changes in cell concentration, percent phytoplankton carbon, or percent primary production.

4.1. Mode-water eddies

The thickness of 18°C subtropical mode water varies due to mesoscale eddy activity (Talley and Raymer, 1982; Ebbesmeyer and Lindstrom, 1986; Brundage and Dugan, 1986). Mode-water eddies form lens shaped isopycnal surfaces, have anticyclonic rotation, and a positive SLA. They displace the seasonal thermocline upward, and displace the main thermocline downward.

There were three mode-water eddy events observed in this time series; they passed the BATS site in May 1993 (May93), July 1995 (Jul95), and October 1995 (Oct95). Each eddy formed lens shaped isopycnal surfaces (Fig. 6b). Both the May93 and Jul95 eddies passed the site when they were less than 2 months old, and corresponded with a significant biological response in the BATS data. They were accompanied by increased rates of primary production to levels nearly as high as the spring blooms (Fig. 5), increased nutrient concentrations at the base of the euphotic zone (Fig. 7), increased pigment concentrations (Figs. 8 and 9), and a shift in phytoplankton community structure to include over a 7-fold increase in the contribution of diatoms to chlorophyll *a* in Jul95 (Fig. 10). Pelagophytes and prasinophytes increased in the May93 event and dinoflagellates became significantly elevated in the Jul95 event. Interestingly, the contribution of *Synechococcus* to total chlorophyll *a* drops to nearly zero in both of these eddies. Only the Jul95 event showed elevated thorium flux. Also, the Jul95 eddy passed over

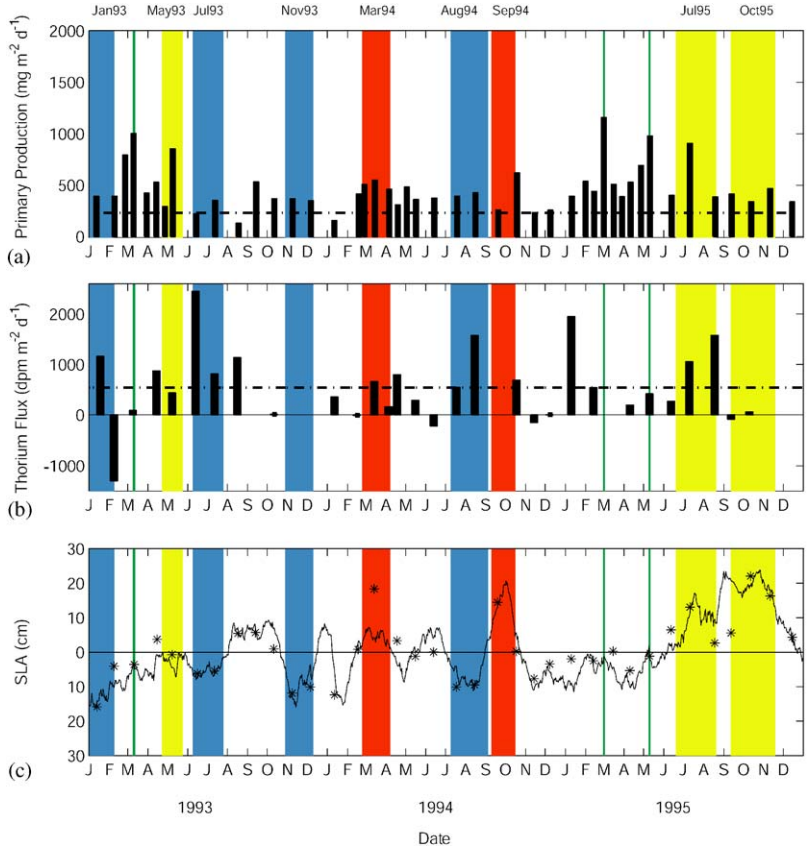

Fig. 5. Integrated primary productivity ($mg\,m^{-2}\,d^{-1}$) (a), ^{234}Th flux ($dpm\,m^{-2}\,d^{-1}$) (b), and SLA at BATS sampling site [black line] and dynamic height [asterisks] (c). Dashed horizontal lines indicate the average value during this study $-230\,mg\,C\,m^{-2}\,d^{-1}$ (a) and $540\,dpm\,m^{-2}\,d^{-1}$ (b). Colored bars indicate eddies: blue—cyclone, yellow—mode-water, and red—anticyclone. Green vertical bars indicate increases in primary productivity that are not associated with eddies.

the site during the same time that sampling by the Bermuda Testbed Mooring (BTM) was occurring (Dickey et al., 1998). The resulting pulse of nutrients and the increased biological response have been documented by McNeil et al. (1999). The failure to observe increased nutrient concentrations in discrete bottle data shown in Fig. 7 for the Jul95 eddy is likely due to inertial oscillations occurring in the water column that depressed the depth of nutrients during the single July BATS measurement (McNeil et al., 1999). This eddy was also identified by Siegel et al. (1999) in their analysis of the thickness of 18°C water (see Fig. 10 in Siegel et al., 1999). The Oct95 event, however, did not show a biological response. It arrived at the time-series site approximately 3–4 months after its formation, much later in the eddy's life than the previous two events.

The observations outlined above indicate the May93 event to be an intensifying eddy with increased nutrients and increased primary production and pigment concentrations. This was the youngest eddy observed in the study (1–1.5 months), and it corresponds to position 3 in the conceptual model. Because the Jul95 event, a slightly older eddy (1.5–3 months), was accompanied by elevated thorium flux we suggest it is at stage 4 in the model. Finally, the Oct95 eddy (aged 3–4 months) did not exhibit a manifestation in primary production, species composition, or export. The upper ocean nitrate signal is problematic due to the erratic pattern of the $0.1\,mmol\,m^{-3}$

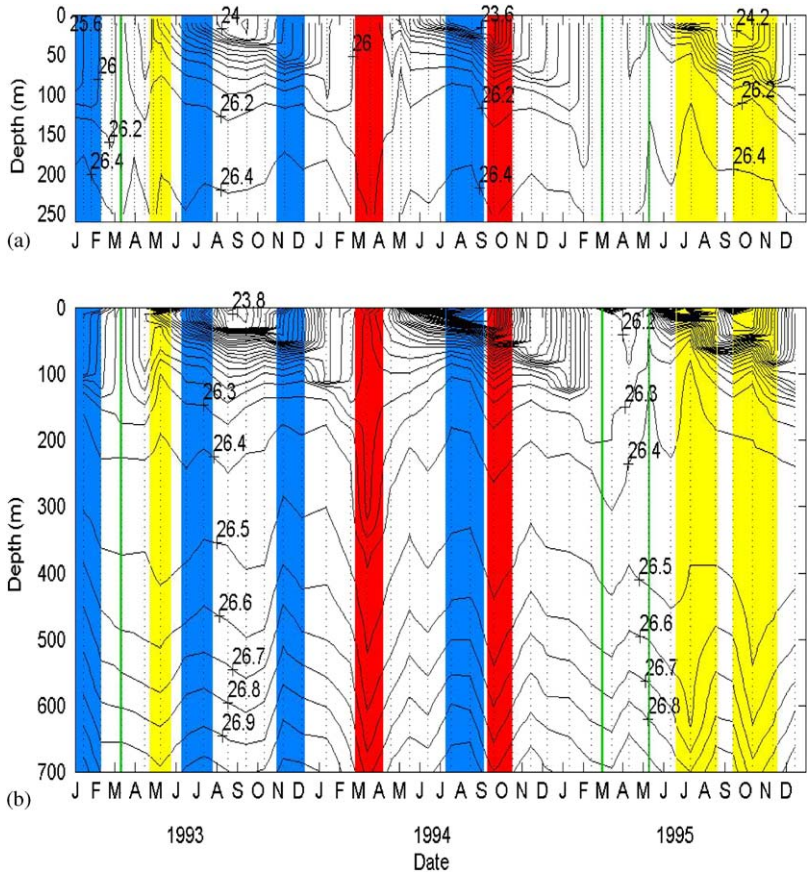

Fig. 6. Sigma theta (kg m^{-3}) in the top 250 m (a) based on BATS "bloom" and "core" cruises and sigma theta from zero to 700 m (b) based on bats "core" cruises only. Colored bars as in Fig. 5. Dots indicate the dates in situ measurements were made.

isoline. However, the general trend of the deeper nitrate surfaces is downward, suggestive of a decreasing trend in upper ocean nitrate concentrations. We therefore classify this eddy as stage 7 in the conceptual model.

From these limited observations it appears that, in the area of Bermuda, a significant impact on biogeochemical indicators occurs as the result of mode-water eddies. This includes increased primary production, a species shift towards larger phytoplankton, and a subsequent high-flux event. The stage in the conceptual model varies for each event from relatively early in the evolution in May93, to well developed in Jul95, and then with the Oct95 event occurring after the biogeochemical response is over and no impact was apparent in the properties analyzed herein.

4.2. Cyclones

Cyclonic eddies are cold-water anomalies that displace isopycnal surfaces upwards and can upwell nutrients into the euphotic zone. There were four cyclones that passed the BATS site during our time series: January 1993 (Jan93), July 1993 (Jul93), November 1993 (Nov93), and August 1994 (Aug94). None of the cyclones showed elevated primary production; however, increased thorium flux and a community structure shift towards greater percentages of *Synechococcus* occurred in Jan93, Jul93, and Aug94. Since the eddies were all at later stages in their "lives" (2–4 months) as compared to the Jul95 and May93 mode-water eddies (1–3 months), the high flux measurements may be the result of a previous

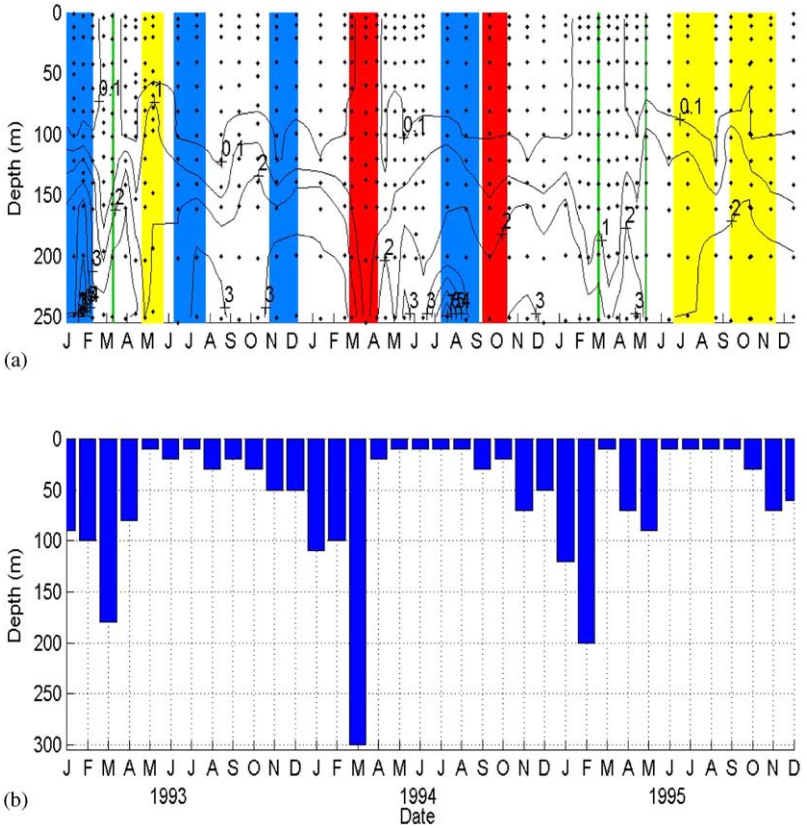

Fig. 7. Nitrate + nitrite (μmol kg^{-1}) in the top 250 m (a), and monthly average mixed layer depth (b). Colored bars as in Fig. 5. Dots in panel (a) indicate the date and sample depth of measurements. The mixed layer depth shown in panel (b) was based on a change of 0.05 kg m^{-3} sigma theta from the surface value.

bloom that occurred as the eddy intensified prior to reaching the sampling site (stage 6). The Nov93 feature showed no response. Unfortunately, a thorium flux measurement is not available for that month. Because the eddy was very old (10 months), we classify it as a stage-7 eddy.

Both cyclones and mode-water eddies produce upwelling of nutrients; however, the observations in the cyclones differed in many ways from the mode-water eddies. First, none of these cyclones were sampled in their first month, making a comparison with the mode-water eddies difficult. However the Aug94 cyclone was similar in many respects to the Jul95 mode-water eddy. Both passed the site in July and August; the cyclone being 2–3 months old and the mode-water eddy being 1.5–3 months old. The cyclone did not show the same increase in productivity and community shift towards larger phytoplankton as the mode-water eddy. This could have been due to the sampling location, which occurred in the western edge of the cyclone and in the center of the mode-water eddy. Unfortunately, biogeochemical gradients within the eddies are not resolvable with the present data set. Alternatively, these variations could reflect a difference in the impacts of cyclones and mode-water eddies on phytoplankton community structure. In these data, cyanobacteria were prevalent in all the cyclones, whereas the mode-water eddies favored a combination of diatoms, dinoflagellates, prasinophytes and pelagophytes. To determine more information about the effects of mode-water eddies and cyclones on the biogeochemistry, and especially this potential

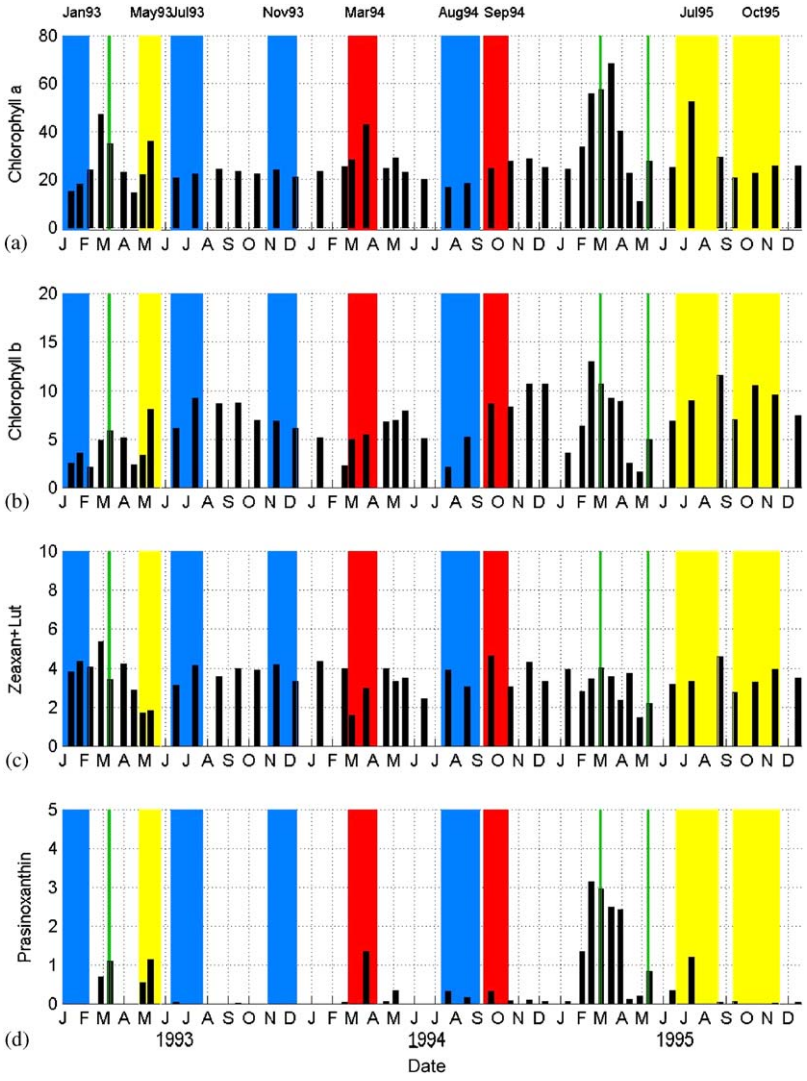

Fig. 8. Depth-integrated (0–250 m) pigment concentrations (mg m^{-2})—chlorophyll *a* (a), chlorophyll *b* (b), zeaxanthin + lutein (c), and prasinoxanthin (d). Colored bars as in Fig. 5.

difference in phytoplankton community structure, it will be necessary to sample the three-dimensional physical, biological, and chemical structure of several of these features at various stages throughout their lifetimes.

4.3. *Anticyclones*

An anticyclone is a warm-water anomaly that depresses the isopycnals and is expected to downwell surface water. It therefore is not expected to cause an increase in biological activity. Two anticyclones are discussed below: March 1994 (Mar94) and September 1994 (Sept94). Both anticyclones can be seen in the depression of the isopycnals (Fig. 6). The Sept94 event showed no notable change from the average conditions at BATS during the early fall; as expected, no major biogeochemical perturbation was associated with the passage of this eddy.

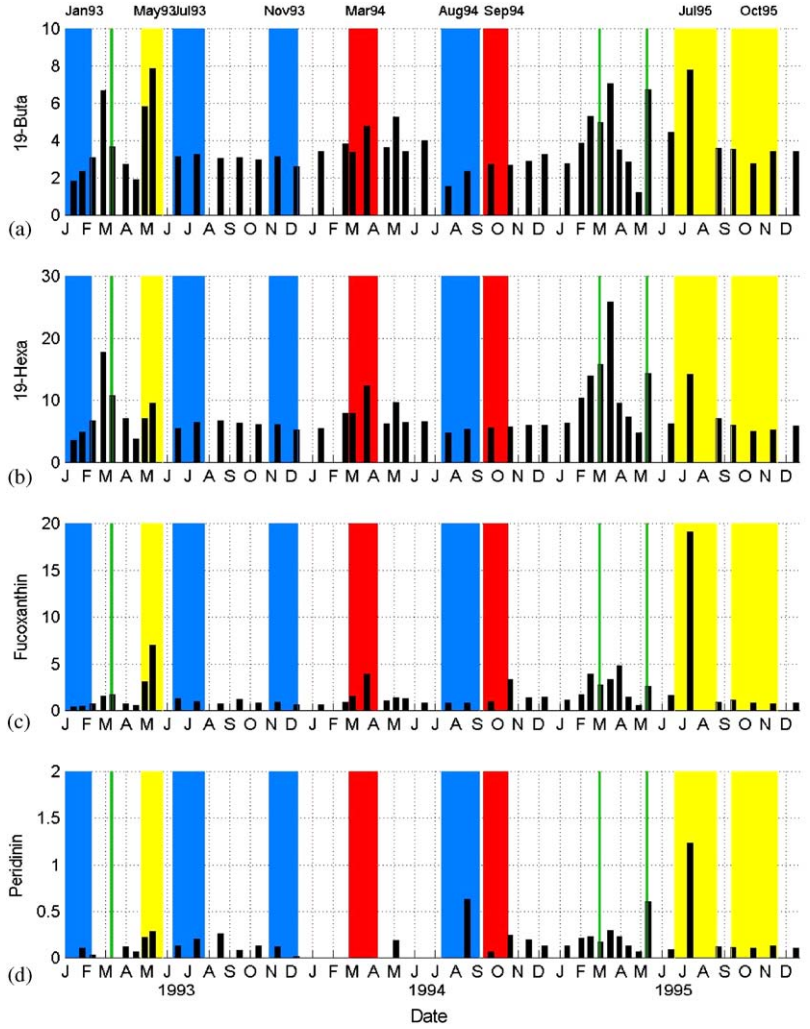

Fig. 9. Depth-integrated (0–250 m) pigment concentrations (mg m^{-2})—19′-butanoyloxyfucoxanthin (a), 19′-hexanoyloxyfucoxanthin (b), fucoxanthin (c), and peridinin (d). Colored bars as in Fig. 5.

The Mar94 event coincided with the 1994 spring bloom at BATS and suppressed the bloom; here the observations in 1994 are presented and compared to the other two spring blooms observed during our study period. For the purpose of this discussion, the spring bloom is the increased primary productivity observed after the seasonal winter entrainment mixing that occurs in the Sargasso Sea. The spring peaks in productivity that occurred during the 1993 and 1995 blooms are marked by narrow green lines (Figs. 5–10). Though indicated by a thin line, these blooms last for days to weeks, and probably impact measurements from multiple BATS cruises both before and after the indicated lines.

Seasonal deep mixing occurred in late February and March of 1993 at the Bermuda site; this is evident in vertical isopycnals in the contour plot of sigma theta (Fig. 6) and in the mixed-layer depth of approximately 180 m (Fig. 7b). The nitrate + nitrite level were also elevated at the surface from late February through March.

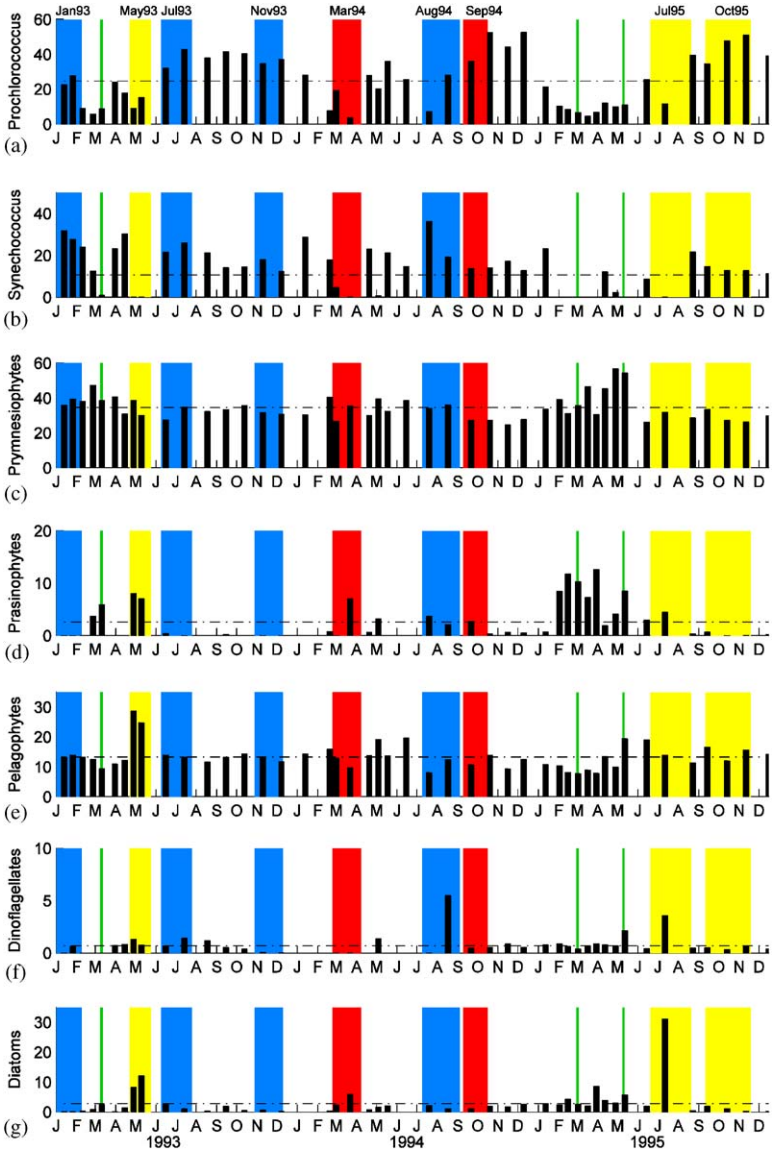

Fig. 10. Species composition (% chlorophyll *a*) of *Prochlorococcus* (a), *Synechococcus* (b), prymnesiophytes (c), prasinophytes (d), pelagophytes (e), dinoflagellates (f), and diatoms (g). Colored bars as in Fig. 5. Dashed horizontal lines indicate the average values during this study—25 (a), 11 (b), 35 (c), 2.5 (d), 13 (e), 1 (f), and 3% (g).

The spring bloom that accompanied this deep mixing event was evidenced by increased primary production rates and increased concentrations of many photosynthetic pigments (Figs. 5, 8, and 9). The 1995 spring bloom followed the same pattern as observed in 1993. Vertical isopycnals and deep mixing occurred in February and March, with deep mixing extending to 200 m in February (Fig. 7). Also, nitrate + nitrite concentrations at the surface were elevated from mid-January to early April, and concentrations were higher than those observed during the 1993 bloom. The phytoplankton pigment concentrations were elevated from February through the end of March. The deeper

mixing in 1995 resulted in a larger nutrient input and was followed by a bloom of longer duration than the 1993 bloom. The species distribution did not shift from a community dominated by nano- and picoplankton, but the prevalence of *Synechococcus* appears to be reduced to near zero during both blooms and prasinophytes seem to thrive under the bloom conditions (Fig. 10). In summary, both the 1993 and 1995 blooms showed increased primary productivity, pigment concentrations elevated in chlorophyll *a*, chlorophyll *b*, prasinoxanthin, 19′-butanoyloxyfucoxanthin, 19′-hexanoyloxyfucoxanthin, fucoxanthin, and peridinin (1995 only), and a community structure dominated by small size class phytoplankton.

In 1994, nutrients were present in the surface but no increased productivity was observed. The productivity during this time was half to one-third the value of the 1993 and 1995 blooms (Fig. 5). The pigment concentrations of chlorophyll *a*, fucoxanthin, 19′-hexanoyloxyfucoxanthin, 19′-butanoyloxyfucoxanthin, and prasinoxanthin were all increased (Figs. 8 and 9), similar to the 1993 and 1995 blooms. The community structure was also similar in that *Synechococcus* diminished and prasinophytes thrived (Fig. 10). This event also was discussed briefly in Michaels and Knap (1996) as an unusually weak spring bloom given the very deep mixed-layer depth. The diminished productivity was likely due to the deep mixing of the organisms out of the euphotic zone during this event. Reduced stratification associated with the eddy's depression of the thermocline appears to have increased the vertical extent of surface-layer mixing, leading to light limitation, and reducing the magnitude of the 1994-bloom event. This illustrates that it is possible for an anticyclone to diminish productivity by overshadowing the spring bloom and suppressing biological responses.

5. Conclusions

5.1. Overview

After discussing each eddy event it is useful to review the time series as a whole. Fig. 5 allows us to view both productivity and export for each event. Of the six flux events over $1000\,\mathrm{dpm\,m^{-2}\,d^{-1}}$, at least four of them were associated with the passage of an eddy, and one was clearly associated with winter mixing (Jan95). For the May93 and Jul95 mode-water eddies, productivity levels were as high as those observed during the 1993 and 1994 spring bloom events. Young mode-water eddies (<2 months) were characterized by a shift towards larger phytoplankton (i.e. diatoms and dinoflagellates) and a drastic decline in the relative abundance of *Synechococcus*. In the oldest of the three mode-water eddies (Oct95), diatoms, dinoflagellates, and *Synechococcus* were present at their typical background levels. In contrast, all four cyclones exhibited an increase in the relative abundance of *Synechococcus*, and in only one case was there a significant increase in large phytoplankton (Aug94 dinoflagellate bloom). These apparent differences in phytoplankton community structure associates with the two types of upwelling eddies (cyclones and mode-water eddies) are tantalizing. However, the present data do not truly resolve such differences, as the time-series record does not include any "young" (less than 2 months old) cyclones. Thus these differences could be explained by eddy age. However, there may be other aspects of these eddies, such as differences in hydrographic properties, seed populations, and food-web dynamics, that modify the effect a particular eddy will have on phytoplankton community structure. Nevertheless, these observations show the significant biological response to eddy perturbations; the temporal aspects of the features are presented in the conceptual model and discussed below.

5.2. The conceptual model

The conceptual model of eddy upwelling (Fig. 2) depicts a mode-water eddy or cyclone as it perturbs an ecosystem. The sequential progression of the conceptual model stages with the ages of the eddies sampled in this study (Fig. 11) suggests that the observations documented herein are consistent with the conceptual model. With intensification, nutrients are upwelled into the euphotic zone where they stimulate a biological response; in these

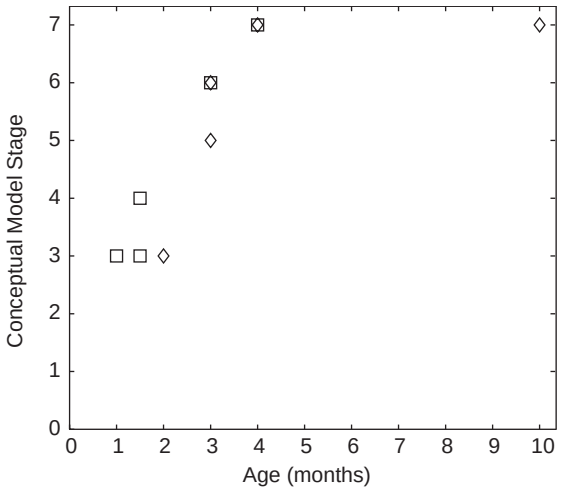

Fig. 11. The conceptual model stage plotted against eddy age (months) for the mode-water (squares) and cyclonic (diamonds) eddies in our study. Eddies with uncertainty in their age or model stage are not shown (see text for details).

observations this occurred in the first 2 months of an eddy's lifetime, as evidenced by events May93 and Jul95. Enhanced biological effects occurred at least as early as month 1.5 and persisted as long as 3 months (events Apr93, May93, Jul94, Aug94, Jul95, Aug95). On decay or relaxation of the eddy, the nutrient addition ends and the biological response diminishes; features greater than 4 months old did not show a biological response (events in Jul93, Nov93, Oct95). The factors that affect the timing of these responses are not understood. This temporal dynamic and its uncertainty complicate the interpretation of the BATS observations. However, we have been able to put the BATS observations into a spatio-temporal context by using satellite altimetry to estimate eddy history and life cycle (i.e. intensification or decay).

Some notable limitations with the simplicity of the conceptual model are worth discussing. First, an eddy's intensity and decay cycle is more complex than depicted in the model, because eddies can increase and decrease intensity multiple times during their life cycle due to eddy–eddy interactions. It is also still unclear how important the age of a feature is to its nutrient injection. Specifically, it is not known if multiple nutrient injections occur and if consecutive injections diminish the intensity of the nutrients. In addition, the importance, extent, and temporal dynamics of eddy "edge effects" are still not known and are not included in the model.

The impact of winter entrainment and deepening of the mixed layer also may affect the biological response to an eddy. High export flux events occurred in both Jan93 (in conjunction with a cyclone) and Jan95 (with no eddy feature present). In order to distinguish eddy impacts from seasonal impacts we need a four-dimensional (space and time) analysis of fluxes and a better understanding of the seasonal cycle in ^{234}Th flux and community structure at BATS. It may be that eddy impacts are most intense during times of seasonal stratification and the establishment of strong nutrient gradients in the upper ocean (Dickey et al., 2001). We observed several eddies during this period (May93, Jul93, Aug94, Jul95), but no young eddies (months 1–3) were observed passing the site during periods when seasonal stratification is absent. More information is needed to determine the importance of stratification.

Finally, we note that this simple conceptual model does not address the observed complexity of the biological response. Whether or not there are systematic differences in phytoplankton community structure associated with nutrient injections from cyclones and mode-water eddies remains to be seen. However, it is clear that highly nonlinear food web dynamics may play a key role in determining plankton species succession and cycling of carbon through the system (e.g. Legendre and Rassoulzadegan, 1996).

5.3. Summary

The results of this study show that eddies exert significant influence on variations in productivity, community structure, and particle flux in the Sargasso Sea. Here we have observed that four out of the six flux events over 1000 dpm m^{-2} d^{-1} during 1993–1995 occurred during the passage of an eddy. The primary productivity was nearly as high as the spring bloom maximum in two of the

three mode-water eddies (May93 and Jul95). The 1994 spring bloom at BATS was significantly depressed by the passage of an anticyclonic eddy. Also, phytoplankton community shifts in mode-water eddies (diatoms and dinoflagellates) and cyclones (*Synechococcus*) were specific and distinct, suggesting that mode-water eddies and cyclones may impact community structure differently. However, until the early impacts of both types of features can be observed, the differences are uncertain. Finally, eddy age appears to explain the presence or absence of a biological response and associated export flux. In general, eddies that were 1–2 months old elicited a large biological response (May93 and Jul95); eddies that were 3 months may show a biological response (Aug94) and were accompanied by high thorium flux (Jul93, Aug94); eddies that were 4 months old or older did not show a biological response or high thorium flux (Nov93 and Oct95).

The conceptual model of eddy upwelling provides a general description of the type of response expected from the passage of an eddy and can explain the observations in the seven upwelling eddies documented here. However, more observations are needed to provide a comprehensive test of the conceptual model. Lagrangian studies that monitor changes following eddy features, high-resolution time-series, and more spatial coverage will all help to provide the needed measurements. With a more complete temporal picture of the effects of eddies, including information about fluxes in four-dimensions, we will significantly improve our understanding of the impacts of mesoscale eddies on biogeochemical cycling in the ocean. Future work may help explain the large observed variability in productivity and particle flux and provide an opportunity to learn more about ecosystem dynamics and controls of community structure.

Acknowledgements

We thank the following individuals for their help with this research: John Andrews, Valery Kosnyrev, Olga Kosnyreva, Scott Doney, Tommy Dickey, David Siegel and Heidi Sosik. We are very grateful for thorough reviews by three referees; their constructive criticism was very useful in improving the manuscript. Support of this activity by NSF and NASA through the JGOFS Synthesis and Modeling Program is greatly appreciated. This is WHOI contribution 10791 and US JGOFS contribution 808.

References

Andersen, R.A., Bidigare, R.R., Keller, M.D., Latasa, M., 1996. A comparison of HPLC pigment signatures and electron microscopic observations for oligotrophic waters of the North Atlantic and Pacific Oceans. Deep-Sea Research II 43, 517–537.

Archer, D., 1995. Upper ocean physics as relevant to ecosystem dynamics: a tutorial. Ecosystem Applications 5 (3), 724–739.

Archiving, Validation, and Interpretation of Satellite Data in Oceanography (AVISO), AVISO handbook: Sea level anomaly files, Publishing AVI-NT-001-312-CN, 21st edition, 24pp (Cent. Nat. d'Etudes Spatiales, Toulouse, France, 1997).

Armstrong, R.A., Lee, C., Hedges, J.I, Honjo, S., Wakeham, S.G., 2002. A new, mechanistic model for organic carbon fluxes in the ocean based on the quantitative association of POC with ballast minerals. Deep-Sea Research II 49 (1–3), 219–236.

Beaulieu, S.E., 2002. Accumulation and fate of phytodetritus on the sea floor. Oceanography and Marine Biology: an Annual Review 40, 171–232.

Benitez-Nelson, C., Buesseler, K.O., Karl, D., Andrews, J., 2001. A time-series study of particular matter export in the North Pacific Subtropical Gyre based upon ^{234}Th: ^{238}U disequilibrium. Deep-Sea Research 48 (12), 2595–2611.

Boyd, P., Newton, P., 1995. Evidence of the potential influence of planktonic community structure on the interannual variability of particulate carbon flux. Deep-Sea Research I 42, 619–639.

Boyd, P.W., Newton, P.P., 1999. Does planktonic community structure determine downward particulate organic carbon flux in different oceanic provinces? Deep-Sea Research I 46, 63–91.

Brundage, W.L., Dugan, J.P., 1986. Observations of an anticyclonic eddy of 18° water in the Sargasso Sea. Journal of Physical Oceanography 16, 717–727.

Brzezinski, M.A., Nelson, D.M., 1995. The annual silica cycle in the Sargasso Sea near Bermuda. Deep-Sea Research I 42, 1215–1237.

Brzezinski, M., Villareal, T., Lipschultz, F., 1998. Silica production and the contribution of diatoms to new and primary production on the central North Pacific. Marine Ecology—Progress Series 167, 89–104.

Buesseler, K.O., 1998. The de-coupling of production and particulate export in the surface ocean. Global Biogeochemical Cycles 12 (2), 297–310.

Buesseler, K.O., Bacon, M.P., Cochran, J.K., Livingston, H.D., 1992a. Carbon and nitrogen export during the JGOFS North Atlantic Bloom Experiment estimated from ^{234}Th: ^{238}U disequilibria. Deep-Sea Research 39, 1115–1137.

Buesseler, K.O., Cochran, J.K., Bacon, M.P., Livingston, H.D., Casso, S.A., Hirschberg, D., Hartman, M.C., Fleer, A.P., 1992b. Determination of thorium isotopes in seawater by non-destructive and radiochemical procedures. Deep-Sea Research Part A 39, 1103–1114.

Buesseler, K.O., Michaels, A.F., Siegel, D.A., Knap, A.H., 1994. A three dimensional time-dependent approach to calibrating sediment trap fluxes. Global Biogeochemical Cycles 8, 179–193.

Buesseler, K., Ball, L., Andrews, J., Benitez-Nelson, C., Belastock, R., Chai, F., Chao, Y., 1998. Upper ocean export of particulate organic carbon in the Arabian Sea derived from thorium-234. Deep-Sea Research II 45, 2461–2487.

Buesseler, K.O., Steinberg, D.K., Michaels, A.F., Johnson, R.J., Andrews, J.E., Valdes, J.R., Price, J.F., 2000. A comparison of the quantity and quality of material caught in a neutrally buoyant versus surface-tethered sediment trap. Deep-Sea Research I 47, 277–294.

Carter, E.F., Robinson, A.R., 1987. Analysis methods for the estimation of oceanic fields. Journal of Atmospheric Oceanic Technology 4, 49–74.

Chen, J.H., Edwards, R.L., Wasserburg, G.J., 1986. ^{238}U, ^{234}U, and ^{232}Th in seawater. Earth and Planetary Science Letters 80, 241–251.

Coale, K., Bruland, K.W., 1987. Oceanic stratified euphotic zone as elucidated by ^{234}Th: ^{238}U disequilibria. Limnology and Oceanography 23, 189–200.

Conte, M.H., Ralph, N., Ross, E.D., 2001. Seasonal and interannual variability in deep ocean particle fluxes at the oceanic flux program (OFP)/Bermuda Atlantic Time Series (BATS) site in the Western Sargasso Sea near Bermuda. Deep-Sea Research II 48, 1471–1505.

Dickey, T., Frye, D., Jannasch, H., Boyle, E., Manov, D., Sigurdson, D., McNeil, J., Stramska, M., Michaels, A., Nelson, N., Siegel, D., Chang, G., Wu, J., Knap, A., 1998. Initial results from the Bermuda Testbed Mooring program. Deep-Sea Research I 45, 771–794.

Dickey, T., Zedler, S., Yu, X., Doney, S.C., Frye, D., Jannasch, H., Manov, D., Sigurdson, D., McNeil, J., Dobeck, L., Gilboy, T., Bravo, C., Siegel, D.A., Nelson, N.B., 2001. Physical and biogeochemical variability from hours to years at the Bermuda Testbed Mooring site: June 1994–March 1998. Deep-Sea Research II 48, 2105–2140.

Doney, S., 1996. A synoptic atmospheric surface forcing data set and physical upper ocean model for the US JGOFS Bermuda Atlantic Time Series (BATS) site. Journal of Geophysical Research 101, 25615–25634.

DuRand, M.D., Olson, R.J., Chisholm, S.W., 2001. Phytoplankton population dynamics at the Bermuda Atlantic time-series station in the Sargasso Sea. Deep-Sea Research II 48 (8–9), 1983–2003.

Ebbesmeyer, C.C., Lindstrom, E.J., 1986. Structure and origin of 18°C water observed during the POLYMODE Local Dynamics Experiment. Journal of Physical Oceanography 16, 443–453.

Fleer, A.P., 1991. Updated determination of particulate and dissolved thorium-234. In: Hurd, D.C., Spencer, D.W. (Eds.), Marine Particles: Analysis and Characterization, Geophysics Monograph Series, 63. AGU, Washington, DC, pp. 227–228.

Francois, R., Honjo, S., Krishfield, R., Manganini, S., 2002. Factors controlling the flux of organic carbon to the bathypelagic zone of the ocean. Global Biogeochemical Cycles 16 (4) 34-1–34-2.

Gardner, W.D., 2000. Sediment trap technology and sampling in surface waters. In: Hanson, R.B., Ducklow, H.W., Field, J.G. (Eds.), The Changing Ocean Carbon Cycle: A Midterm Synthesis of the Joint Global Ocean Flux Study. Cambridge University Press, Cambridge, pp. 240–281.

Glover, H.E., Prézelin, B.B., Campbell, L., Wyman, M., Garside, C., 1988. A nitrate-dependent *Synechococcus* bloom in surface Sargasso Sea water. Nature 331, 161–163.

Goldman, J.C., 1988. Spatial and temporal discontinuities of biological processes in pelagic surface waters. In: Rothschild, B.J. (Ed.), Toward a Theory on Biological–Physical Interactions in the World Ocean. Kluwer Academic, Dordrecht, pp. 273–296.

Goldman, J.C., 1993. Potential role of large oceanic diatoms in new primary production. Deep-Sea Research I 40, 159–168.

Harrison, D., Heinmiller, R., 1983. Upper ocean variability in the Sargasso Sea July 1977–July 1978: the POLYMODE XBT program. Journal of Physical Oceanography 13, 859–872.

Honjo, S., Dymond, J., Prell, W., Ittekkot, V., 1999. Monsoon-controlled export fluxes to the interior of the Arabian Sea. Deep-Sea Research II 42, 831–870.

Jeffrey, S.W., Mantoura, R.F.C., Wright, S.W. (Eds.), 1997. Phytoplankton Pigments in Oceanography: Guidelines to Modern Methods. UNESCO Publishing, Paris, p. 661.

Karl, D.M., Letelier, R., Hebel, D., Tupas, I., Dore, J., Christian, J., Winn, C., 1995. Ecosystem changes in the North Pacific subtropical gyre attributed to the 1991–1992 El Niño. Nature 373, 230–234.

Karl, D.M., Christian, J.R., Dore, J.E., Hebel, D.V., Letelier, R.M., Tupas, L.M., Winn, C.D., 1996. Seasonal and interannual variability in primary production and particle flux at Station aloha. Deep-Sea Research II 43, 539–568.

Knap, A.H., Michaels, A.F., Dow, R.L., Johnson, R.J., Gundersen, K., Sorensen, J.C., Close, A., Howse, F., Hammer, M., Bates, N., Doyle, A., Waterhouse, T., 1993. BATS methods Manual, Version 3. US JGOFS Planning Office, Woods Hole, MA, USA.

Legendre, L., Rassoulzadegan, F., 1996. Food-web mediated export of biogenic carbon in oceans: hydrodynamic control. Marine Ecology Progress Series 145, 179–193.

LeTraon, P.Y., Ogor, F., 1998. ERS-1/2 orbit improvement using TOPEX/POSEIDON: the 2-cm challenge. Journal of Geophysical Research 103, 8045–8050.

LeTraon, P.Y., Gaspar, P., Bouyssel, F., Makhmara, H., 1995. Using TOPEX/POSEIDON data to enhance ERS-1 data. Journal of Atmospheric Oceanic Technology 12, 161–170.

Letelier, R.M., Bidigare, R.R., Hebel, D.V., Ondrusek, M., Winn, C.D., Karl, D.M., 1993. Temporal variability of phytoplankton community structure based on pigment analysis. Limnology and Oceanography 38 (7), 1420–1437.

Letelier, R., Karl, D., Abbott, M., Flament, P., Freilich, M., Lukas, R., 2000. Role of late winter mesoscale events in the biogeochemical variability of the upper water column of the North Pacific Subtropical Gyre. Journal of Geophysical Research 105, 28723–28739.

Lohrenz, S.E., Knauer, G.A., Asper, V.L., Tuel, M., Michaels, A.F., Knap, A.H., 1992. Seasonal and interannual variability in primary production and particle flux in the Northwestern Sargasso Sea: US JGOFS Bermuda Atlantic Time-Series Study. Deep-Sea Research 39, 1373–1391.

Mackey, M.D., Mackey, D.J., Higgins, H.W., Wright, S.W., 1996. CHEMTAX—a program for estimating class abundances from chemical markers: Application to HPLC measurements of phytoplankton. Marine Ecology—Progress Series 144, 265–283.

Mackey, D.J., Higgins, H.W., Mackey, M.D., Holdsworth, D., 1998. Algal class abundances in the western equatorial Pacific: estimation from HPLC measurements of chloroplast pigments using CHEMTAX. Deep-Sea Research I 45, 1441–1468.

McGillicuddy, D.J., Robinson, A.R., 1997. Eddy-induced nutrient supply and new production in the Sargasso Sea. Deep-Sea Research I 44, 1427–1450.

McGillicuddy Jr., D.J., Robinson, A.R., Siegel, D.A., Jannasch, H.W., Johnson, R., Dickey, T.D., McNeil, J., Michaels, A.F., Knap, A.H., 1998. Influence of mesoscale eddies on new production in the Sargasso Sea. Nature 394, 263–265.

McGillicuddy Jr., D.J., Johnson, R., Siegel, D.A., Michaels, A.F., Bates, N.R., Knap, A.H., 1999. Mesoscale variations in biogeochemical properties in the Sargasso Sea. Journal of Geophysical Research 104 (C6), 13381–13394.

McGillicuddy, D.J., Anderson, L.A., Doney, S.C., Maltrud, M.E., 2003. Eddy-driven sources and sinks of nutrients in the upper ocean: results from a 0.1° resolution model of the North Atlantic. Global Biogeochemical Cycles 17 (2), 1035 (doi:10.1029/2002GB001987).

McNeil, J.D., Jannasch, H.W., Dickey, T., McGillicuddy, D., Brzezinski, M., Sakamoto, C.M., 1999. New Chemical, bio-optical and physical observations of upper ocean response to the passage of a mesoscale eddy off Bermuda. Journal of Geophysical Research 104 (C7), 15537–15548.

Michaels, A.F., 1995. Ocean time series research near Bermuda: the Hydrostation S time-series and the Bermuda Atlantic Time-series Study (BATS) program. In: Powell, T.M., Steele, H.J. (Eds.), Ecological Time Series. Chapman & Hall, New York, pp. 181–208.

Michaels, A.F., Knap, A.H., 1996. Overview of the US JGOFS Bermuda Atlantic Time-series Study and the Hydrostation S program. Deep-Sea Research II 43 (2–3), 157–198.

Michaels, A.F., Silver, M.W., 1988. Primary production, sinking fluxes and the microbial food web. Deep-Sea Research 35, 473–490.

Michaels, A.F., Knap, A.H., Dow, R.L., Gundersen, K., Johnson, R.J., Sorensen, J., Close, A., Knauer, G.A., Lohrenz, S.E., Asper, V.A., Tuel, M., Bidigare, R., 1994a. Seasonal patterns of ocean biogeochemistry at the US JGOFS Bermuda Atlantic Time-series Study site. Deep-Sea Research I 41, 1013–1038.

Michaels, A.F., Bates, N.R., Buesseler, K.O., Carlson, C.A., Knap, A.H., 1994b. Carbon system imbalances in the Sargasso Sea. Nature 372, 537–540.

Newton, P.P., Lampitt, R.S., Jickells, T.D., King, P., Boutle, C., 1994. Temporal and spatial variability of biogenic particle fluxes during the JGOFS northeast Atlantic process studies at 47°N, 20°W. Deep-Sea Research I 41, 1617–1642.

Noshkin, V.E., DeAgazio, E., 1966. Low background beta detector for solid sample assay. Nuclear Instrumental Methods 39, 265–270.

Olaizola, M., Ziemann, D., Bienfang, P., Walsh, W., Conquest, L., 1993. Eddy-induced oscillations of the pycnocline affect the floristic composition and depth distribution of phytoplankton in the subtropical Pacific. Marine Biology 116, 533–542.

Oschlies, A., 2002. Can eddies make ocean deserts bloom? Global Biogeochemical Cycles 16 (4) 53-1–53-11.

Oschlies, A., Garcon, V., 1998. Eddy-induced enhancement of primary production in a model of the North Atlantic Ocean. Nature 394, 266–269.

Richman, J.G., Wunsch, C., Hogg, N.G., 1977. Space and time scales of mesoscale motions in the western North Atlantic. Reviews of Geophysics 15, 377–385.

Roman, M.R., Adolf, H.A., Landry, M.R., Madin, L.P., Steinberg, D.K., Zhang, X., 2002. Estimates of oceanic mesozooplankton production: a comparison between the Bermuda and Hawaii time-series data. Deep-Sea Research II 49 (1–3), 175–192.

Savidge, G., Williams, P.le B., 2001. The PRIME 1996 cruise: an overview. Deep-Sea Research II 48, 687–704.

Scharek, R., Latasa, M., Karl, D., Bidigare, R., 1999a. Temporal variations in diatom abundance and downward vertical flux in the oligotrophic north pacific gyre. Deep-Sea Research I 46, 1051–1075.

Scharek, R., Tupas, L., Karl, D., 1999b. Diatom fluxes to the deep sea in the oligotrophic North Pacific gyre at station ALOHA. Marine Ecology—Progress Series 182, 55–67.

Seki, M., Polvina, J., Brainard, R., Bidigare, R., Leonard, C., Foley, D., 2001. Biological enhancement at cyclonic eddies tracked with GOES thermal imagery in Hawaiian waters. Geophysical Research Letters 28, 1583–1586.

Sieburth, J.M., Smetacek, V., 1978. Pelagic ecosystem structure: heterotrophic compartments of the plankton and their relationship to plankton size fractions. Limnology and Oceanography 23, 1256–1263.

Siegel, D.A., McGillicuddy Jr., D.J., Fields, E.A., 1999. Mesoscale eddies, satellite altimetry, and new production in the Sargasso Sea. Journal of Geophysical Research 104 (C6), 13359–13379.

Silver, M.W., Gowing, M.M., Davoll, P.J., 1986. The association of photosynthetic picoplankton and ultraplankton with pelagic detritus through the water column (0–2000 m). Canadian Bulletin of Fisheries and Aquatic Sciences 214, 311–341.

Steinberg, D.K., Carlson, C.A., Bates, N.R., Johnson, R.J., Michaels, A.F., Knap, A.H., 2001. Overview of the US JGOFS Bermuda Atlantic Time-series Study (BATS): a decade-scale look at ocean biology and biogeochemistry. Deep-Sea Research II 48, 1405–1447.

Sweeney, E.N., 2001. Monthly variability in upper ocean biogeochemistry due to mesoscale eddy activity in the Sargasso Sea, Master's Thesis, Massachusetts Institute of Technology, Cambridge, MA, 02139, and Woods Hole Oceanographic Institution, Woods Hole, MA, 02543, unpublished.

Takahashi, M., Bienfang, P.K., 1983. Size-structure of phytoplankton biomass and photosynthesis in subtropical Hawaiian waters. Marine Biology 76, 203–211.

Talley, L.D., Raymer, M.E., 1982. Eighteen degree water variability. Journal of Marine Research 40, 757–775.

The MODE Group, 1978. The mid-ocean dynamics experiment. Deep-Sea Research 25, 859–910.

Wiebe, P., Joyce, T., 1992. Introduction to interdisciplinary studies of Kuroshio and Gulf Stream Rings. Deep Sea Research 39, S1–S6.

Wright, S.W., van den Enden, R.L., 2000. Phytoplankton community structure and stocks in the East Antarctic marginal ice zone (BROKE survey, January–March 1996) determined by CHEMTAX analysis of HPLC pigment signatures. Deep-Sea Research II 47, 2363–2400.